# Size-dependent catalytic activity of monodispersed nickel nanoparticles for the hydrolytic dehydrogenation of ammonia borane

Kun Guo[a,b], Hailong Li[c] and Zhixin Yu[a,b]*

[a] *Department of Petroleum Engineering, University of Stavanger, 4036 Stavanger, Norway*

[b] *The National IOR Centre of Norway, University of Stavanger, 4036 Stavanger, Norway*

[c] *Department of Energy, Building and Environment, Mälardalen University, 72123 Västerås, Sweden*

*Corresponding author:

Zhixin Yu:

Tel.: +47 51 83 22 38;

Fax: +47 51 83 20 50;

E-mail: zhixin.yu@uis.no

**Calculation method of the TOF:**

Given that some of our Ni NPs fall in a relatively large size domain, e.g., the 13.3, 18.8 and 27.4 nm Ni NPs, we calculate the TOF by assuming that only the Ni atoms located in the outermost 5 nm layer of the highly dispersed NP are active in the liquid phase reaction system.[1] The ratio ($R$) of active Ni atoms in each NP can be calculated as the equation below:

$$R = 1 - \frac{\frac{4}{3}\pi\left(\frac{d_{Ni} - 5}{2}\right)^3}{\frac{4}{3}\pi\left(\frac{d_{Ni}}{2}\right)^3} = 1 - (\frac{d_{Ni} - 5}{d_{Ni}})^3$$

where $d_{Ni}$ is the diameter of Ni NP. For the 4.9 nm Ni NPs, $R$ equals one. The calculation of TOF is thus given as the equation below:

$$TOF = \frac{V_{H_2}}{22.4 * V_s * C_{Ni} * t * R}$$

where $V_{H_2}$ is the total volume of $H_2$ generated, $V_s$ is the volume of solution, $C_{Ni}$ is the molar concentration of Ni NPs added in the reaction mixture, and $t$ is the reaction time.[2-4]

**Table S1**. The SSAs of three carbon materials given by the suppliers and measured in this study.

| Carbon materials | SSA given by the suppliers | SSA measured in this study |
|---|---|---|
| **KB** | 1400 $m^2 \cdot g^{-1}$ | 1339.3 $m^2 \cdot g^{-1}$ |
| **CNT** | 100−160 $m^2 \cdot g^{-1}$ | 113.8 $m^2 \cdot g^{-1}$ |
| **GNP** | 50−80 $m^2 \cdot g^{-1}$ | 62.5 $m^2 \cdot g^{-1}$ |

**Table S2**. Average particle sizes and crystal sizes of the Ni NPs measured from the TEM and XRD characterizations.

| Average particle size from TEM | Average crystal size from XRD[a] |
|---|---|
| 27.4 nm | 7.4 nm |
| 18.8 nm | 5.6 nm |
| 13.3 nm | 4.3 nm |
| 8.9 nm | 3.9 nm |
| 4.9 nm | 2.8 nm |

[a] Calculation based on the (111) crystal plane using the Scherrer equation

**Table S3**. The TOFs of different carbon supported catalysts and unsupported 8.9 nm Ni NPs.

| Catalyst | TOF ($mol_{H_2} \cdot mol_{Ni}^{-1} \cdot h^{-1}$) |
|---|---|
| **8.9 nm Ni/KB** | 357.7 |
| **8.9 nm Ni/CNT** | 199.3 |
| **8.9 nm Ni/GNP** | 220.8 |
| **8.9 nm Ni NPs** | 154.2 |

**Table S4**. Catalytic activity in terms of TOF of the reported metal-based catalysts for the hydrolytic dehydrogenation of AB.

| Catalyst | TOF[a] ($mol_{H_2} \cdot mol_{Ni}^{-1} \cdot h^{-1}$) | Reference |
|---|---|---|
| **4.9 nm Ni/KB** | 447.9 | this study |
| **Skeletal Ni** | 318 | [5] |
| **PVP stabilized Ni** | 270 | [6] |
| **3.2 nm Ni/KB** | 528 | [7] |
| **Hollow Ni NPs** | 258 | [8] |
| **Ag@Ni/graphene** | 462 | [9] |
| **Pd/zeolite** | 375 | [10] |
| **Pd/hydroxyapatite** | 300 | [11] |
| **Cu@Co/graphene** | 501.6 | [12] |
| **Cu@FeNi** | 502.2 | [13] |
| **Ag/C/Ni** | 319.2 | [14] |
| **CuCo/graphene** | 588.6 | [15] |
| **$Ru_1Cu_{7.5}$/graphene** | 588 | [16] |

| | | |
|---|---|---|
| **Co/zeolite** | 321.6 | [17] |
| **Cu/zeolite** | 47 | [18] |
| **Co/graphene oxide** | 289.8 | [19] |
| **In-situ Fe** | 150 | [20] |
| **Ni/$Al_2O_3$** | 390 | [21] |
| **Cu@$SiO_2$** | 194.4 | [22] |
| **PEG stabilized Fe** | 384 | [23] |
| **Co@N-C-700** | 336 | [24] |
| **PtNi@$SiO_2$** | 332.4 | [25] |

[a] Values either recalculated or directly provided based on the original data in the studies

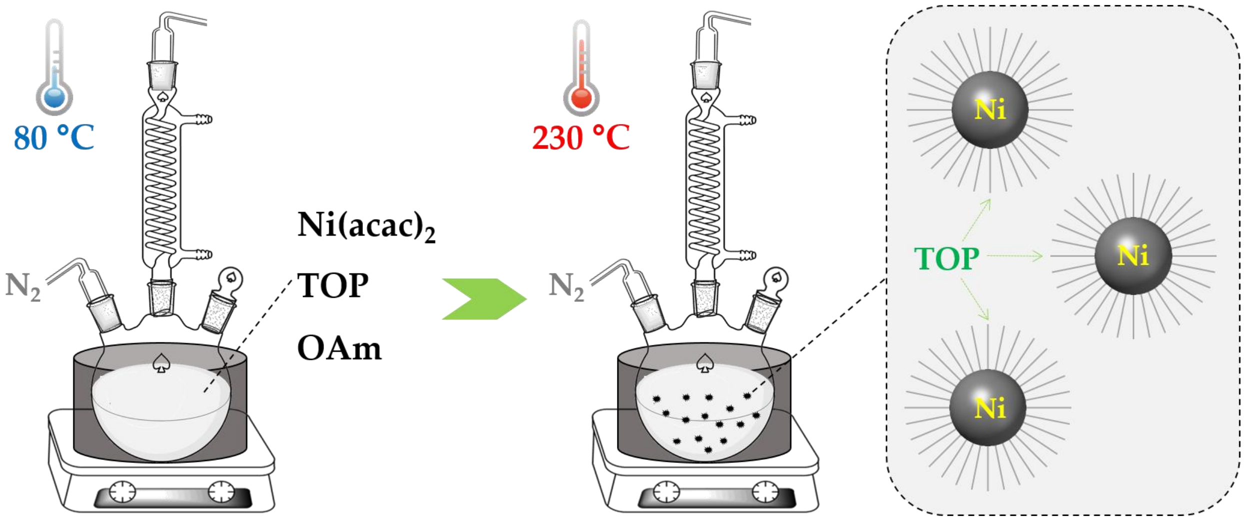


**Scheme S1**. Schematic illustration of the synthetic procedures of monodispersed Ni NPs.

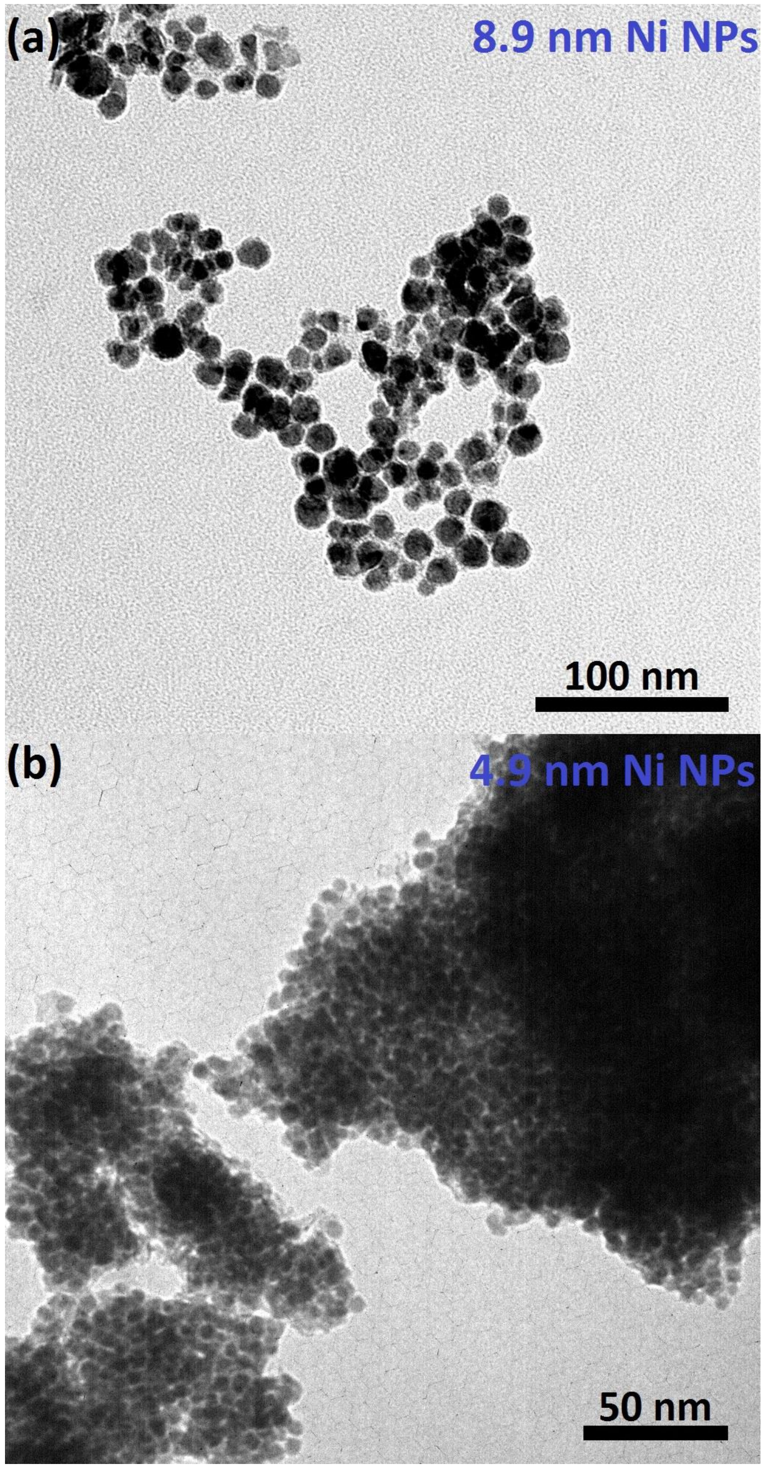


**Figure S1**. Representative TEM images of the spent (a) 8.9 and (b) 4.9 nm Ni NPs after the dehydrogenation of AB.

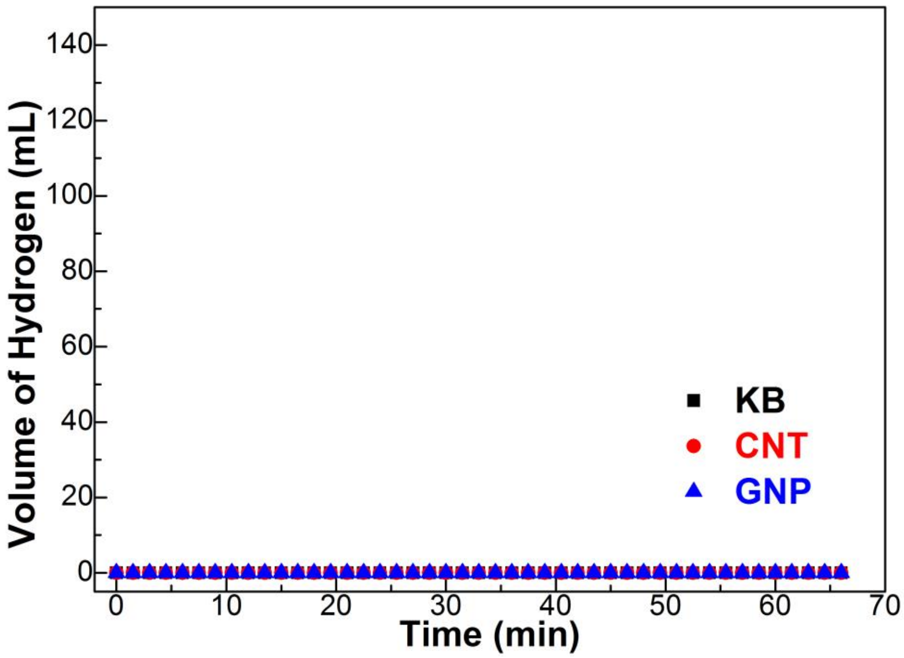


**Figure S2**. Blank experiments of the dehydrogenation of AB with three carbon supports.

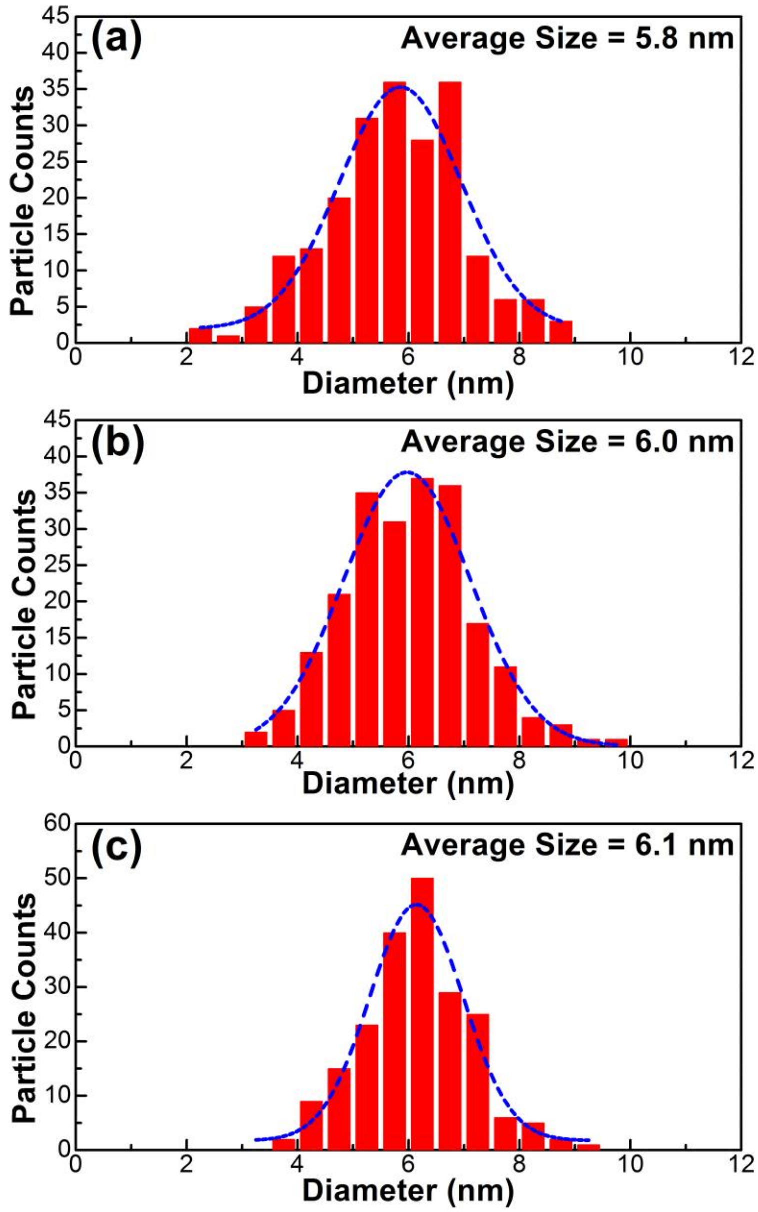


**Figure S3**. PSD curves with Gaussian fits of the 4.9 nm Ni/KB catalyst before the test (a), after five catalytic cycles (b), and after the New-1$^{st}$ cycle (c).

## References


(1) Guo, L. L.; Gu, X. J.; Kang, K.; Wu, Y. Y.; Cheng, J.; Liu, P. L.; Wang, T. S.; Su, H. Q. Porous Nitrogen-Doped Carbon-Immobilized Bimetallic Nanoparticles as Highly Efficient Catalysts for Hydrogen Generation from Hydrolysis of Ammonia Borane. *J. Mater. Chem. A* 2015, 3 (45), 22807−22815.

(2) Yao, Q. L.; Lu, Z. H.; Huang, W.; Chen, X. S.; Zhu, J. High Pt-like Activity of the Ni-Mo/Graphene Catalyst for Hydrogen Evolution from Hydrolysis of Ammonia Borane. *J. Mater. Chem. A* 2016, 4 (22), 8579−8583.

(3) Liu, P.; Gu, X.; Kang, K.; Zhang, H.; Cheng, J.; Su, H. Highly Efficient Catalytic Hydrogen Evolution from Ammonia Borane Using the Synergistic Effect of Crystallinity and Size of Noble-Metal-Free Nanoparticles Supported by Porous Metal-Organic Frameworks. *ACS Appl. Mater. Interfaces* **2017,** *9* (12), 10759−10767.

(4) Ge, Y.; Ye, W.; Shah, Z. H.; Lin, X.; Lu, R.; Zhang, S. PtNi/NiO Clusters Coated by Hollow Sillica: Novel Design for Highly Efficient Hydrogen Production from Ammonia-Borane. *ACS Appl. Mater. Interfaces* **2017,** *9* (4), 3749−3756.

(5) Nozaki, A.; Tanihara, Y.; Kuwahara, Y.; Ohmichi, T.; Mori, K.; Nagase, T.; Yasuda, H. Y.; Yamashita, H. Skeletal Ni Catalysts Prepared from Amorphous Ni-Zr Alloys: Enhanced Catalytic Performance for Hydrogen Generation from Ammonia Borane. *Chemphyschem* **2016,** *17* (3), 412−417.

(6) Umegaki, T.; Yan, J. M.; Zhang, X. B.; Shioyama, H.; Kuriyama, N.; Xu, Q. Preparation and Catalysis of Poly(N-Vinyl-2-Pyrrolidone) (PVP) Stabilized Nickel Catalyst for Hydrolytic Dehydrogenation of Ammonia Borane. *Int. J. Hydrogen Energy* **2009,** *34* (9), 3816−3822.

(7) Metin, O.; Mazumder, V.; Ozkar, S.; Sun, S. Monodisperse Nickel Nanoparticles and Their Catalysis in Hydrolytic Dehydrogenation of Ammonia Borane. *J. Am. Chem. Soc.* **2010,** *132* (5), 1468−1469.

(8) Umegaki, T.; Yan, J.-M.; Zhang, X.-B.; Shioyama, H.; Kuriyama, N.; Xu, Q. Hollow Ni–$SiO_2$ Nanosphere-Catalyzed Hydrolytic Dehydrogenation of Ammonia Borane for Chemical Hydrogen Storage. *J. Power Sources* **2009,** *191* (2), 209−216.

(9) Yang, L.; Luo, W.; Cheng, G. Graphene-Supported Ag-Based Core-Shell Nanoparticles for Hydrogen Generation in Hydrolysis of Ammonia Borane and Methylamine Borane. *ACS Appl. Mater. Interfaces* **2013,** *5* (16), 8231−8240.

(10) Rakap, M.; Ozkar, S. Zeolite Confined Palladium(0) Nanoclusters as Effective and Reusable Catalyst for Hydrogen Generation from the Hydrolysis of Ammonia-Borane. *Int. J. Hydrogen Energy* **2010,** *35* (3), 1305−1312.

(11) Rakap, M.; Ozkar, S. Hydroxyapatite-Supported Palladium(0) Nanoclusters as Effective and Reusable Catalyst for Hydrogen Generation from the Hydrolysis of Ammonia-Borane. *Int. J. Hydrogen Energy* **2011,** *36* (12), 7019−7027.

(12) Du, Y. S.; Cao, N.; Yang, L.; Luo, W.; Cheng, G. Z. One-Step Synthesis of Magnetically Recyclable rGO Supported Cu@Co Core-Shell Nanoparticles: Highly Efficient Catalysts for Hydrolytic Dehydrogenation of Ammonia Borane and Methylamine Borane. *New J. Chem.* **2013,** *37* (10), 3035−3042.

(13) Wang, H. L.; Yan, J. M.; Wang, Z. L.; Jiang, Q. One-Step Synthesis of Cu@FeNi Core-Shell Nanoparticles: Highly Active Catalyst for Hydrolytic Dehydrogenation of Ammonia Borane. *Int. J. Hydrogen Energy* **2012,** *37* (13), 10229−10235.

(14) Wen, M.; Sun, B. L.; Zhou, B.; Wu, Q. S.; Peng, J. Controllable Assembly of Ag/C/Ni Magnetic Nanocables and Its Low Activation Energy Dehydrogenation Catalysis. *J. Mater. Chem.* **2012,** *22* (24), 11988−11993.

(15) Yan, J. M.; Wang, Z. L.; Wang, H. L.; Jiang, Q. Rapid and Energy-Efficient Synthesis of a Graphene-CuCo Hybrid as a High Performance Catalyst. *J. Mater. Chem.* **2012,** *22* (22), 10990−10993.

(16) Cao, N.; Hu, K.; Luo, W.; Cheng, G. Z. RuCu Nanoparticles Supported on Graphene: A Highly Efficient Catalyst for Hydrolysis of Ammonia Borane. *J. Alloys Compd.* **2014,** *590*, 241−246.

(17) Rakap, M.; Ozkar, S. Hydrogen Generation from the Hydrolysis of Ammonia-Borane Using Intrazeolite Cobalt(0) Nanoclusters Catalyst. *Int. J. Hydrogen Energy* **2010,** *35* (8), 3341−3346.

(18) Zahmakıran, M.; Durap, F.; Özkar, S. Zeolite Confined Copper(0) Nanoclusters as Cost-Effective and Reusable Catalyst in Hydrogen Generation from the Hydrolysis of Ammonia-Borane. *Int. J. Hydrogen Energy* **2010,** *35* (1), 187−197.

(19) Hu, J.; Chen, Z.; Li, M.; Zhou, X.; Lu, H. Amine-Capped Co Nanoparticles for Highly Efficient Dehydrogenation of Ammonia Borane. *ACS Appl. Mater. Interfaces* **2014,** *6* (15), 13191−13200.

(20) Yan, J. M.; Zhang, X. B.; Han, S.; Shioyama, H.; Xu, Q. Iron-Nanoparticle-Catalyzed Hydrolytic Dehydrogenation of Ammonia Borane for Chemical Hydrogen Storage. *Angew. Chem. Int. Ed.* **2008,** *47* (12), 2287−2289.

(21) Metin, O.; Ozkar, S.; Sun, S. H. Monodisperse Nickel Nanoparticles Supported on $SiO_2$ as an Effective Catalyst for the Hydrolysis of Ammonia-Borane. *Nano Res.* **2010,** *3* (9), 676−684.

(22) Yao, Q.; Lu, Z. H.; Zhang, Z.; Chen, X.; Lan, Y. One-Pot Synthesis of Core-Shell Cu@$SiO_2$ Nanospheres and Their Catalysis for Hydrolytic Dehydrogenation of Ammonia Borane and Hydrazine Borane. *Sci. Rep.* **2014,** *4*, 7597.

(23) Dinç, M.; Metin, Ö.; Özkar, S. Water Soluble Polymer Stabilized Iron(0) Nanoclusters: A Cost-Effective and Magnetically Recoverable Catalyst in Hydrogen Generation from the Hydrolysis of Sodium Borohydride and Ammonia Borane. *Catal. Today* **2012,** *183* (1), 10−16.

(24) Wang, H. X.; Zhao, Y. R.; Cheng, F. Y.; Tao, Z. L.; Chen, J. Cobalt Nanoparticles Embedded in Porous N-Doped Carbon as Long-Life Catalysts for Hydrolysis of Ammonia Borane. *Catal. Sci. Technol.* **2016,** *6* (10), 3443−3448.

(25) Qi, X.; Li, X.; Chen, B.; Lu, H.; Wang, L.; He, G. Highly Active Nanoreactors: Patchlike or Thick Ni Coating on Pt Nanoparticles Based on Confined Catalysis. *ACS Appl. Mater. Interfaces* **2016,** *8* (3), 1922−1928.